

# “Click” Synthesis of Thermally Stable Au Nanoparticles with Highly Grafted Polymer Shell and Control of Their Behavior in Polymer Matrix

JONGMIN LIM,<sup>1</sup> HYUNSEUNG YANG,<sup>1</sup> KWANYEOL PAEK,<sup>1</sup> CHUL-HEE CHO,<sup>1</sup> SEYONG KIM,<sup>2</sup> JOONA BANG,<sup>2</sup> BUMJOON J. KIM<sup>1</sup>

<sup>1</sup>Department of Chemical and Biomolecular Engineering, Korea Advanced Institute of Science and Technology, Daejeon 305-701, Republic of Korea

<sup>2</sup>Department of Chemical and Biological Engineering, Korea University, Seoul 136-701, Republic of Korea

Received 9 April 2011; accepted 16 May 2011

DOI: 10.1002/pola.24782

Published online 8 June 2011 in Wiley Online Library (wileyonlinelibrary.com).

**ABSTRACT:** Thermally stable core-shell gold nanoparticles (Au NPs) with highly grafted polymer shells were synthesized by combining reversible addition-fragmentation transfer (RAFT) polymerization and click chemistry of copper-catalyzed azide-alkyne cycloaddition (CuAAC). First, alkyne-terminated poly(4-benzylchloride-*b*-styrene) (alkyne-PSCI-*b*-PS) was prepared from the alkyne-terminated RAFT agent. Then, an alkyne-PSCI-*b*-PS chain was coupled to azide-functionalized Au NPs via the CuAAC reaction. Careful characterization using FT-IR, UV-Vis, and TGA showed that PSCI-*b*-PS chains were successfully grafted onto the Au NP surface with high grafting density. Finally, azide groups were introduced to PSCI-*b*-PS chains on the Au NP surface to produce thermally stable Au NPs with crosslinkable polymer shell (Au-PSN<sub>3</sub>-*b*-PS 1). As the control sample, PS-*b*-PSN<sub>3</sub>-coated Au NPs (Au-PSN<sub>3</sub>-*b*-PS 2) were made by the conventional “grafting to” approach. The

grafting density of polymer chains on Au-PSN<sub>3</sub>-*b*-PS 1 was found to be much higher than that on Au-PSN<sub>3</sub>-*b*-PS 2. To demonstrate the importance of having the highly packed polymer shell on the nanoparticles, Au-PSN<sub>3</sub>-*b*-PS 1 particles were added into the PS and PS-*b*-poly(2-vinylpyridine) matrix, respectively. Consequently, it was found that Au-PSN<sub>3</sub>-*b*-PS 1 nanoparticles were well dispersed in the PS matrix and PS-*b*-P2VP matrix without any aggregation even after annealing at 220 °C for 2 days. Our simple and powerful approach could be easily extended to design other core-shell inorganic nanoparticles. © 2011 Wiley Periodicals, Inc. *J Polym Sci Part A: Polym Chem* 49: 3464–3474, 2011

**KEYWORDS:** block copolymers; click chemistry; grafting density; nanocomposites; nanoparticles; polymer coated Au nanoparticles; reversible addition fragmentation chain transfer (RAFT)

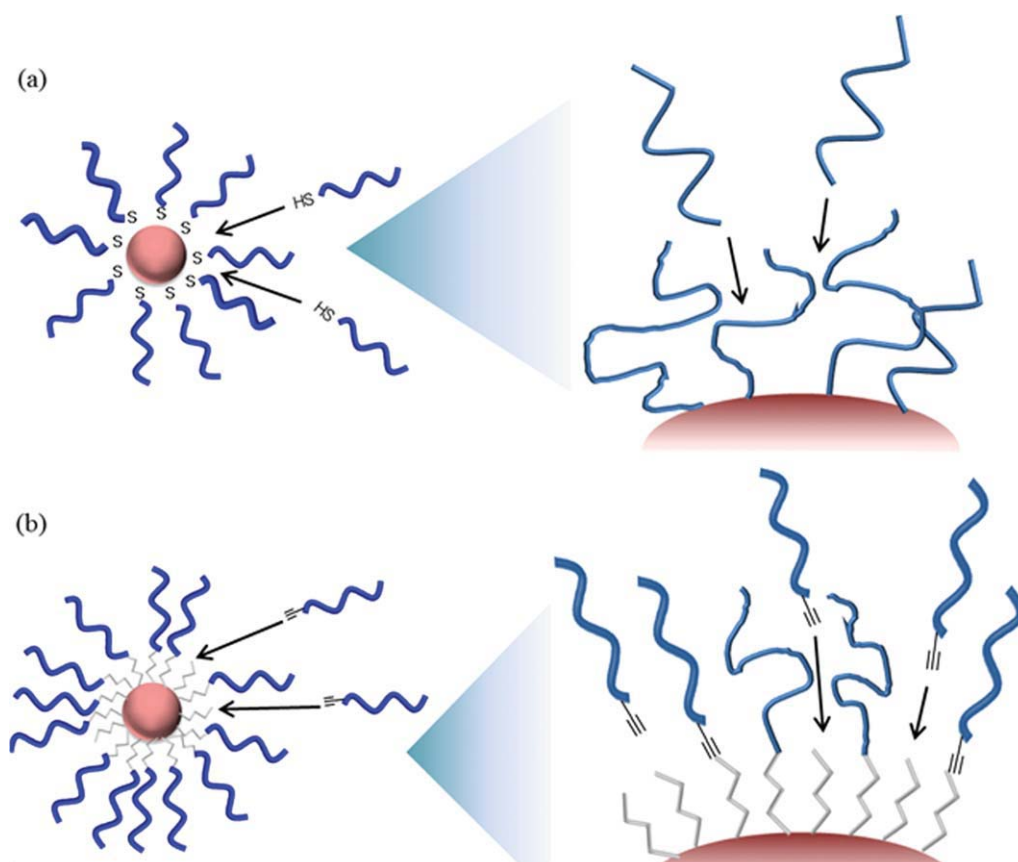
**INTRODUCTION** Polymer-inorganic hybrid materials have been the subject of intense research recently because of their potentials in various applications, including high performance optical and energy devices,<sup>1,2</sup> microelectronics,<sup>3,4</sup> data storage,<sup>5,6</sup> and highly selective membranes.<sup>7,8</sup> Incorporation of inorganic nanoparticles into polymer matrices can combine the functionality of nanoparticles with easy processability of polymers. However, achieving the ordered structure or dispersing the nanoparticles within the polymer matrix is usually challenging, particularly because of the inherent immiscibility between inorganic particles and organic materials.<sup>9</sup> To address these issues, there have been some approaches to control the interaction between nanocrystals and polymer chains within a matrix by manipulating the interface between the nanoparticle surface and the polymer matrix. One of the most powerful methods to improve the chemical affinity of nanoparticles is to design the proper polymeric ligands that can be grafted on the surfaces of inorganic particles. For example, tuning the surface properties of nanoparticles by end-attaching ligands such as organic small

molecules,<sup>10–15</sup> a single type or a mixture of homopolymers,<sup>16–24</sup> random copolymers,<sup>25</sup> and block copolymers<sup>7,26,27</sup> to the nanoparticle surface can position the particles precisely at the interface between two different polymers. In this manner, the particles would have surfactant-like properties in a block copolymer or polymer matrix.<sup>25,28</sup> In the block copolymer matrix, the interaction between the polymer shell on the particles and the chains in the block copolymer matrix determines not only the dispersion of particles in the matrix but also controls their location within the matrix.

There are two principle pathways for producing inorganic core-polymeric shell type nanoparticles. In the “grafting to” approach [Scheme 1(a)], presynthesized ligands with functional end groups that interact favorably with the nanoparticle surfaces are simply bound to the vacant sites during the particle formation step.<sup>29,30</sup> The presynthesized ligands can also substitute other ligands that were originally on the particle surface via the ligand exchange step.<sup>31,32</sup> A wide range of presynthesized polymers with great control in the molecular weight, polydispersity, and molecular structure, is

Correspondence to: J. Bang (E-mail: joona@korea.ac.kr) or B. J. Kim (E-mail: bumjoonkim@kaist.ac.kr)

*Journal of Polymer Science Part A: Polymer Chemistry*, Vol. 49, 3464–3474 (2011) © 2011 Wiley Periodicals, Inc.



**SCHEME 1** Comparison of the (a) grafting-to and (b) click approach for controlling grafting density of polymers on Au NPs.

accessible for the grafting to approach. However, the main limitation of this method rests with the fact that the achievable polymer surface density on the nanoparticles is low because of the steric hindrance that prevents additional polymers to approach the surfaces. On the other hand, the “grafting from” method can overcome this drawback and induce much higher grafting density of the polymer ligands on nanoparticle surfaces. However, it should be noted that this approach typically requires more complex procedures to synthesize polymer-coated nanoparticles and allows much less control in the polymer ligand characteristics, such as the molecular weight, the polydispersity, and the molecular structure. More importantly, most of the radical polymerization procedures, including the controlled radical polymerization process, typically require the temperature to be above 60 °C. At this temperature, many metallic nanoparticles (i.e., gold, silver, platinum) stabilized by thiol-functionalized ligands become thermally unstable and form aggregates because of the breakage of particle surface–ligand bondings.<sup>33</sup> Therefore, an alternative strategy is still necessary to produce polymer-coated nanoparticles with a high grafting density.

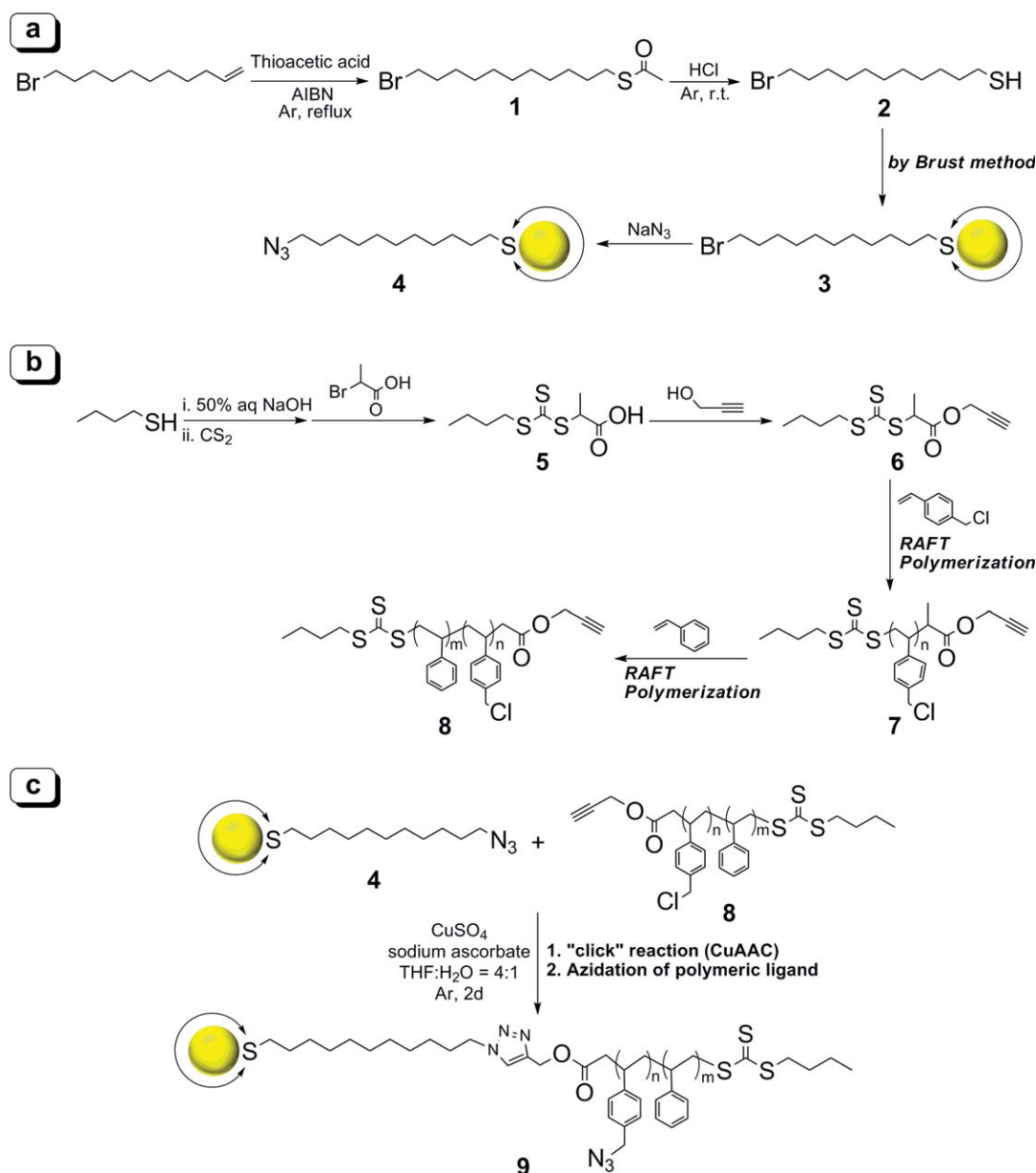
Emerged as the premier example of “click” chemistry,<sup>34,35</sup> copper-catalyzed azide-alkyne cycloaddition (CuAAC) is a technique that has been extensively used in copolymer synthesis,<sup>36,37</sup> surface functionalization,<sup>38,39</sup> and bioconjugations.<sup>40</sup>

This simple and robust reaction can produce intended products in very high yields with almost no byproduct, and it also works well under mild conditions.<sup>41</sup> In addition, several research groups have suggested the use of the click chemistry approach for the functionalization of 2D and 3D substrates, including the functionalization of nanoparticles.<sup>42–48</sup> For example, Fleming et al.<sup>45</sup> synthesized azide-functionalized Au NPs coupled with various alkyne derivatives. Boisselier et al. demonstrated the click addition of hydrophilic polyethyleneoxide (PEO) on Au NPs using CuSO<sub>4</sub> as a catalyst under a mixture of water and tetrahydrofuran (THF). Very recently, Drockenmuller et al.<sup>46</sup> reported the synthesis of PEO- or poly(caprolactone)-coated Pt nanoparticles by click chemistry. These examples showed that the surfaces of Au NPs could be effectively decorated by polymers using the CuAAC reaction. However, most work on the click synthesis of polymer coated Au NPs were limited to using water-soluble polymers including PEO and poly(N-isopropylacrylamide) (PNIPAM) as the surface ligands because of the solubility issues. Another important problem was that the copper catalyst in the click reaction results in aggregation of nanoparticles and/or low yield.<sup>44,45</sup>

Herein, we combine the CuAAC reaction with the “grafting-to” approach to produce inorganic nanoparticles with a densely packed polymer shell [Scheme 1(b)]. Properly

designed diblock copolymer of polystyrene (PS) and poly(4-benzylchloride) (PSCI) with an alkyne end group was first synthesized by reversible addition-fragmentation transfer (RAFT) polymerization (Scheme 2). Subsequently, it was coupled to azide-functionalized Au NPs (Au-N<sub>3</sub>) by the CuAAC reaction to produce Au NPs with a highly grafted polymer shell. To achieve an efficient click reaction between hydrophobic polymers and Au-N<sub>3</sub> without aggregation of nanoparticle, the ratio of THF/water in the reaction was carefully optimized so that all reagents including catalyst and salt were dissolved and the reaction could be completed. We chose PS-*b*-poly(azidostyrene) (PS-*b*-PSN<sub>3</sub>) diblock copolymers as ligands for two reasons. First, PS-*b*-

PSN<sub>3</sub> diblock copolymer shell on Au NPs could be easily crosslinked to enhance the thermal stability of the Au NPs as shown in the previous report.<sup>49</sup> Second, previous examples of nanoparticle surface functionalization using the CuAAC reaction were mostly limited to hydrophilic systems. Because PS-*b*-PSN<sub>3</sub> diblock copolymers have extremely low solubility in water, it can be demonstrated that our approach to produce polymer-coated Au NPs with highly grafted PS-*b*-PSN<sub>3</sub> shells was very versatile and could be easily extended to other hydrophobic systems. In addition, we discussed the behavior of the Au NPs with highly packed polymer shell in homopolymer and diblock copolymer matrix.



**SCHEME 2** Synthesis scheme for thermally stable Au NPs with densely packed diblock copolymer shell via the click reaction. Synthesis procedure for (a) Au-N<sub>3</sub>, (b) alkyne-PSCI-*b*-PS block copolymers, and (c) Au-PSN<sub>3</sub>-*b*-PS 1 nanoparticles via the CuAAC reaction. [Color figure can be viewed in the online issue, which is available at [wileyonlinelibrary.com](http://wileyonlinelibrary.com).]

## RESULTS AND DISCUSSION

## Synthesis of Thermally Stable Au NPs with Highly Grafted Polymer Shell via Click Chemistry and RAFT Polymerization

Au-N<sub>3</sub> nanoparticles were synthesized following the processes shown in Scheme 2(a). First, 11-bromo-1-undecanethiol **2** was synthesized via a two-step reaction from 11-bromo-1-undecene. Then, the unique peak [acetyl group (2.3 ppm)] of compound **1** completely disappeared. Instead, a peak at 2.49 ppm appeared because of the presence of the thiol group at the end of compound **2** (Fig. 1). Using compound **2** as ligand, bromine-functionalized Au NPs (Au-Br) were successfully prepared by the Brust method. The NMR spectrum of Au-Br in Figure 1(d) shows the peak around 3.4 ppm, a signature of the bromine end group. It was noted that compared to the sharp peak from the molecule **2**, NMR peaks of the Au NPs were significantly broadened because of the ligand attached at the particle surface.<sup>50,51</sup> The Au-Br nanoparticles were then stirred in a solution containing NaN<sub>3</sub> to convert the Br-termini on the Au NP surface into the azide (N<sub>3</sub>) group via nucleophilic substitution. It was found that the core size and shape of Au-N<sub>3</sub> particles were not affected during this reaction, and the particle core diameter was 2.51 nm as shown in the transmission electron microscope (TEM) image of Figure 2(a). The presence of azide functional groups on the Au NP surface was evidenced by NMR and FTIR measurements. In the NMR spectrum, a broad peak that previously appeared around 3.4 ppm shifted completely to 3.24 ppm because of azide substitution [Fig. 1(e)]. The FTIR spectrum in Figure 3(a) shows a strong signal at 2100 cm<sup>-1</sup>, which is a signature of the azide groups. Therefore, it can be concluded

that Au NPs were completely functionalized by azide end groups.

Azide groups on the Au NP surface enabled further functionalization via CuAAC reaction with alkyne derivatives. Therefore, two different alkyne end-functionalized PS (alkyne-PS 1 and alkyne-PS 2) and alkyne-terminated PStCl-*b*-PS block copolymers (alkyne-PStCl-*b*-PS) were prepared by RAFT polymerization, as shown in Scheme 2(b). Alkyne-terminated RAFT chain transfer agent **6** was designed and prepared according to the modified literature procedure to ensure the functionality required for the click chemistry.<sup>52,53</sup> The molecular weight ( $M_n$ ) and polydispersity index (PDI) of alkyne-PStCl-*b*-PS were found to be 8.8 kg/mol and 1.1, respectively, with PStCl ( $M_n = 3.3$  kg/mol) and PS ( $M_n = 5.5$  kg/mol) blocks. Two additional alkyne-PS 1 and alkyne-PS 2 were synthesized to have different  $M_n$ . The  $M_n$  and PDI of alkyne-PS 1 were 4.5 kg/mol and 1.07, respectively, and the  $M_n$  and PDI of alkyne-PS 2 were 12 kg/mol and 1.1, respectively. The information for all polymers is summarized in Table 1.

The previous examples of grafting polymers on Au NPs using the CuAAC reaction suffered from low yield and/or nanoparticle aggregation mainly because of the different solubilities of the different reagents including the polymers, the Au NPs, the catalyst, and the salts.<sup>44,45,48</sup> This could also cause a serious problem of lowering the grafting density of the polymer shell on the Au NPs and limit the usefulness of the CuAAC reaction on the nanoparticles. To overcome such problems, the CuAAC reaction conditions in this system were first optimized by coupling two model polymers, alkyne-PS 2 and PS-*b*-PSN<sub>3</sub> polymers, without using Au NPs. In this case, the corresponding copolymers could be readily recovered and the molecular weight could be easily traced via size exclusion

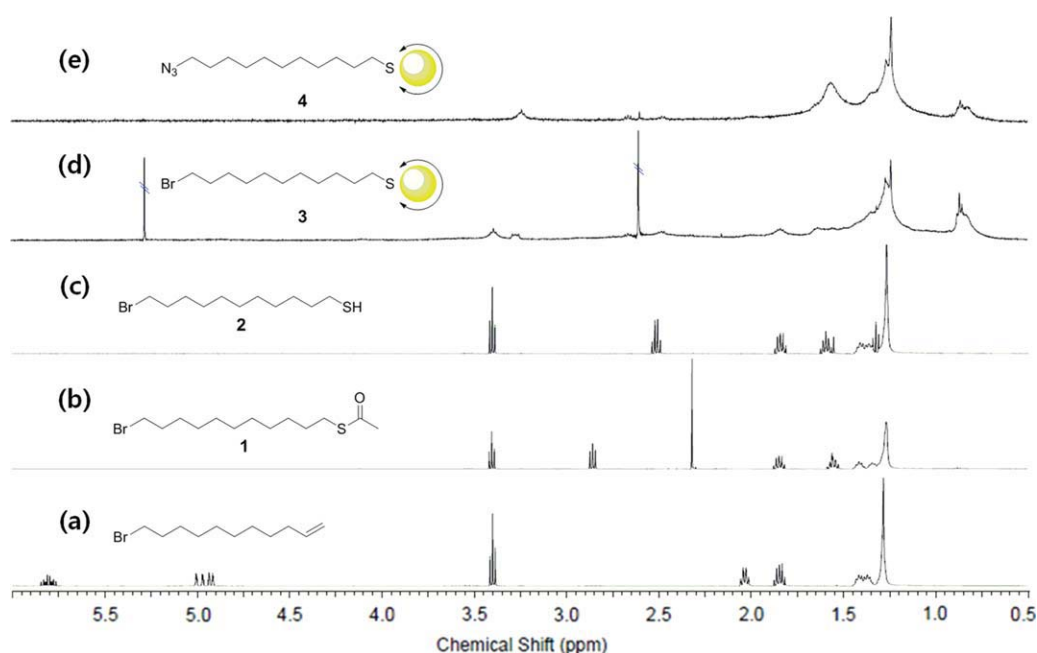


**FIGURE 1** NMR spectra of (a) 11-bromo-1-undecene, (b) 11-(bromoundecyl)thioacetate, (c) 11-bromo-1-undecanethiol, (d) Au-Br, and (e) Au-N<sub>3</sub>. [Color figure can be viewed in the online issue, which is available at [wileyonlinelibrary.com](http://wileyonlinelibrary.com).]

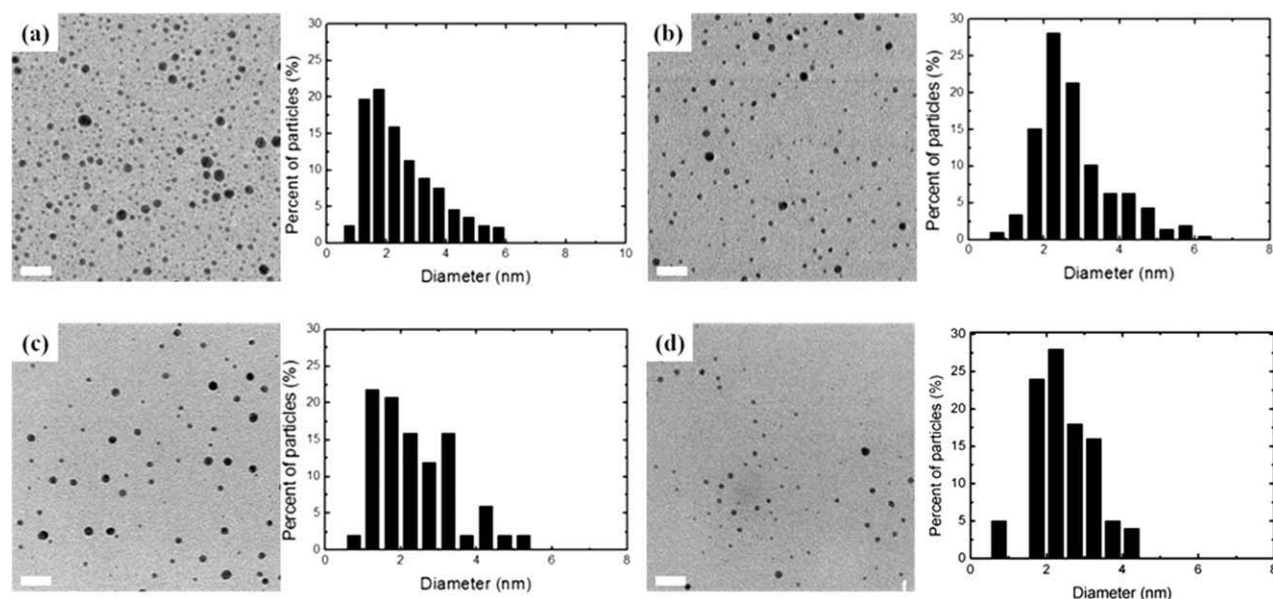


**FIGURE 2** TEM images of Au NPs and the corresponding histograms of their size distribution: (a) Au-N<sub>3</sub> (2.51 ± 1.19 nm), (b) Au-PS (2.79 ± 1.03 nm), (c) Au-PSN<sub>3</sub>-*b*-PS 1 (click; 2.37 ± 1.01 nm), and (d) Au-PSN<sub>3</sub>-*b*-PS 2 (grafting-to; 2.48 ± 0.74 nm). Scale bar is 20 nm.

chromatography (SEC). To monitor the efficiency of the CuAAC reaction, the PS-*b*-PSN<sub>3</sub> polymer was designed to be monodisperse with only a few units of the azide group per each chain. The total  $M_n$  of PS-*b*-PSN<sub>3</sub> was 5.4 kg/mol. It should be noted that there are, on average, four units of the

azide group per each chain (PSN<sub>3</sub>  $M_n$  = 0.7 kg/mol). After surveying the reaction efficiency with a variety of Cu catalysts, such as CuBr, CuI, CuSO<sub>4</sub>, salts, and solvents, it was found that the system of CuSO<sub>4</sub>/sodium ascorbate/(THF/water) gave the best results with a reaction yield close to completion. It should be noted that the solvent mixture ratio (THF/water) was an important parameter because sodium ascorbate requires water to be dissolved. However, both PS-*b*-PSN<sub>3</sub> and alkyne-PS 2 showed extremely low solubility in water. Figure 4 shows the SEC curves of the polymers after the CuAAC reaction between PS-*b*-PSN<sub>3</sub> and a slight excess amount of alkyne-PS 2 under different THF-to-water ratio. The SEC curve in Figure 4(c) shows a peak at 12 kg/mol for alkyne-PS 2, which indicates that no reaction occurred. As the ratio of THF to water increased from 1:8 to 1:4 and to 1:1, the peak at the lower retention time ( $M_n$  = 56 kg/mol) appeared. Interestingly, this number of  $M_n$  = 56 kg/mol corresponded approximately to the total molecular weights for one PS-*b*-PSN<sub>3</sub> chain ( $M_n$  = 5.4 kg/mol) and four alkyne-PS 2 chains ( $M_n$  = 12 kg/mol). The number of alkyne-PS 2 chains was consistent with the average number of azide

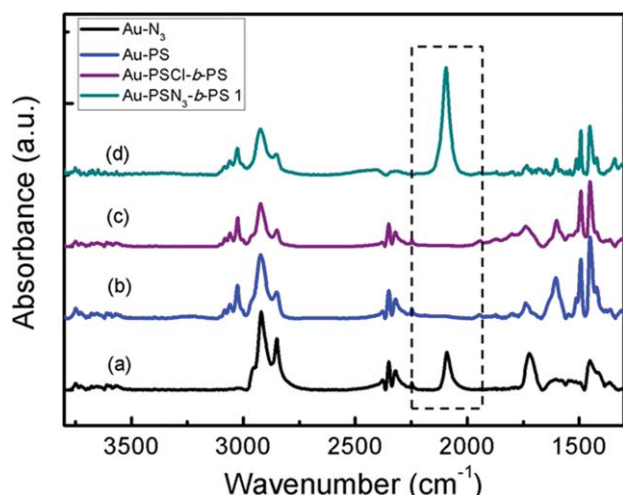


**FIGURE 3** FTIR spectra of synthesized Au NPs. (a) Au-N<sub>3</sub>, (b) Au-PS, (c) Au-PSCI-*b*-PS, and (d) Au-PSN<sub>3</sub>-*b*-PS 1. In (a), the peak at ~2100 cm<sup>-1</sup> represents the presence of the azide group on the Au NP surface. In (b) and (c), after the click reaction between the azide group on the Au NPs and the alkyne group at the end of alkyne-PSCI-*b*-PS chain, the peak at ~2100 cm<sup>-1</sup> disappeared, which indicates the efficient click reaction. In (d), the azide peak reappeared after azidation of PSCI-*b*-PS polymer brushes on the Au NPs, (PS-Cl → PS-N<sub>3</sub>). [Color figure can be viewed in the online issue, which is available at [wileyonlinelibrary.com](http://wileyonlinelibrary.com).]

**TABLE 1** Characteristics of Polymers Used in This Study

Polymer	$M_n$ (kg/mol)	PDI
Alkyne-PS 1	4.5	1.07
Alkyne-PS 2	12	1.10
Alkyne-PSCI- <i>b</i> -PS	8.8	1.10
PS- <i>b</i> -PSN <sub>3</sub>	5.4	1.09
PS- <i>b</i> -PSN <sub>3</sub> -SH	8.7	1.07
PS	56.5	1.07
PS- <i>b</i> -P2VP	380	1.10

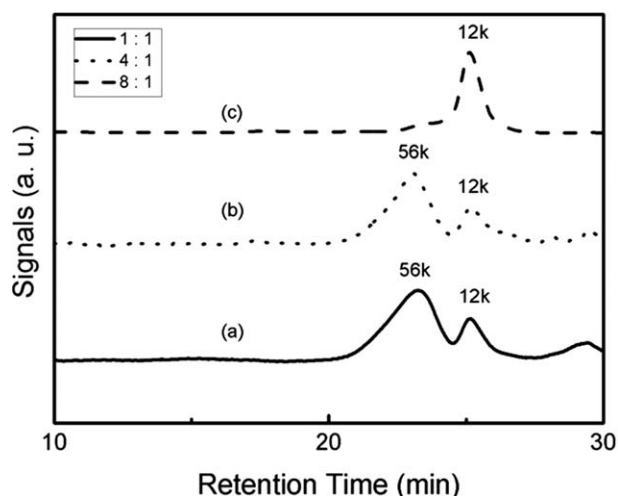


**FIGURE 4** SEC curves of the polymers after the CuAAC reaction between PS-*b*-PSN<sub>3</sub> chains and alkyne-PS 2 chains under different THF/water ratio. (a) THF:water = 1:1 (v/v), (b) THF:water = 4:1 (v/v), and (c) THF:water = 8:1 (v/v).

groups in a PS-*b*-PSN<sub>3</sub> chain (four units of the azide group in each chain). Additionally, there was no peak between the two peaks of  $M_n = 12$  and 56 kg/mol, which indicates the completion of the CuAAC reaction between two different polymers.

These conditions were used for the main CuAAC reaction between Au-N<sub>3</sub> particles and alkyne polymers. As a result, two different particles of PS-coated Au NPs (Au-PS) and PS-*b*-PSN<sub>3</sub>-coated Au NPs (Au-PSN<sub>3</sub>-*b*-PS 1) were synthesized. For the case of Au-PSN<sub>3</sub>-*b*-PS 1, additional azide substitution was performed on PS-*b*-PSCI-coated Au NPs. To monitor the efficiency of the CuAAC reaction and the extent of attachment of the polymers on Au NPs, FTIR spectra of each type of Au NPs were taken (Fig. 3). Comparison between Au-N<sub>3</sub> and polymer-coated Au NPs revealed that the strong signal of the azide group at 2100 cm<sup>-1</sup> disappeared after the CuAAC reaction. Although additional peaks above 3000 cm<sup>-1</sup> in Figure 3(b,c) appeared due to the C-H stretching vibration of the aromatic ring, alkyl stretching vibrations between 2800 and 3000 cm<sup>-1</sup> of the polymer-coated Au NPs were consistent with the pristine Au-N<sub>3</sub>. This indicates that the structures of the compounds were not affected by surface attachment. PS chains were successfully grafted on the Au

NP surface via click reaction of terminal alkynes in PS chains with the azides on the Au NPs. Figure 3(d) shows that the azide peak for the Au-PSN<sub>3</sub>-*b*-PS 1 particles reappeared. This clearly indicates that the chlorine groups in PSCI units were successfully replaced with azide groups by reacting PS-*b*-PSCI chains on the Au NPs with NaN<sub>3</sub>, producing Au-PSN<sub>3</sub>-*b*-PS 1.

All synthesized Au NPs were analyzed by TEM to obtain the core size and the grafting density of polymers on the Au NPs. The information for all Au NPs is listed in Table 2. Figure 2 represents the TEM images of four different Au NPs. The core diameters of (a) Au-N<sub>3</sub>, (b) Au-PS, and (c) Au-PSN<sub>3</sub>-*b*-PS 1 were almost all around 2.5 nm, which indicates that the particle size was not affected by the CuAAC reaction. Interestingly, the TEM images in Figure 2 provide qualitative support for the increase in the shell thickness by polymer ligands. In this case, the interparticle distance between Au NPs dispersed on the carbon film on the TEM grid was significantly larger for Au-PS and Au-PSN<sub>3</sub>-PS 1 than for Au-N<sub>3</sub> particles, which indicates that the PS shell on the Au particle core was much thicker and consistent with the previous report.<sup>54</sup> The areal density of polymer chains grafted onto the Au NPs is an important parameter to determine the efficiency of the click reaction on the synthesis of polymer-coated Au NPs. The areal chain density ( $\Sigma$ ) of each Au NP was calculated based on the gold core size from TEM and the weight fraction of gold and polymer ligands in the core-shell Au NPs from thermogravimetric analysis (TGA). The details of the method were described in the Experimental section. The  $\Sigma$  of Au-PS was estimated to be 2.23 chains/nm<sup>2</sup>, which was much higher than what can be obtained from the “grafting-to” method using PS chains with a similar molecular weight synthesized by RAFT polymerization.<sup>55</sup> In the “grafting-to” method case,  $\Sigma$  values were always less than 1.6 chains/nm<sup>2</sup> because of the secondary position of thiol groups. For a higher molecular weight polymer ligand, such as alkyne-PSCI-*b*-PS ( $M_n = 8.8$  kg/mol), the  $\Sigma$  of Au-PSN<sub>3</sub>-*b*-PS 1 was estimated to be 1.22 chains/nm<sup>2</sup>. To prove the significance of the click reaction on Au-PSN<sub>3</sub>-*b*-PS 1 particles, another sample of PS-*b*-PSN<sub>3</sub>-coated Au NPs (Au-PSN<sub>3</sub>-*b*-PS 2) was made by the conventional grafting-to approach as the control sample.<sup>17,25,49</sup> Thiol-terminated PS-*b*-PSN<sub>3</sub> (PS-*b*-PSN<sub>3</sub>-SH) was synthesized by RAFT polymerization to have the  $M_n$  of 8.7 kg/mol and the PDI of 1.07, respectively. It was noted that the  $M_n$  of this polymer was similar to that

**TABLE 2** Size and Grafting Density of Polymer-Grafted Au NPs by the Click Chemistry Approach and the Grafting-to Approach

	Particle Core Diameter (nm)	Particle (Core + Shell) Diameter (nm)	Grafting Density $\Sigma$ (chains/nm <sup>2</sup> )	Method
Au-N <sub>3</sub>	2.51	5.20	7.79	–
Au-PS	2.79	9.14	2.23	Click
Au-PSN <sub>3</sub> - <i>b</i> -PS 1	2.37	8.36	1.22	Click
Au-PSN <sub>3</sub> - <i>b</i> -PS 2	2.48	7.79	0.90	Grafting-to

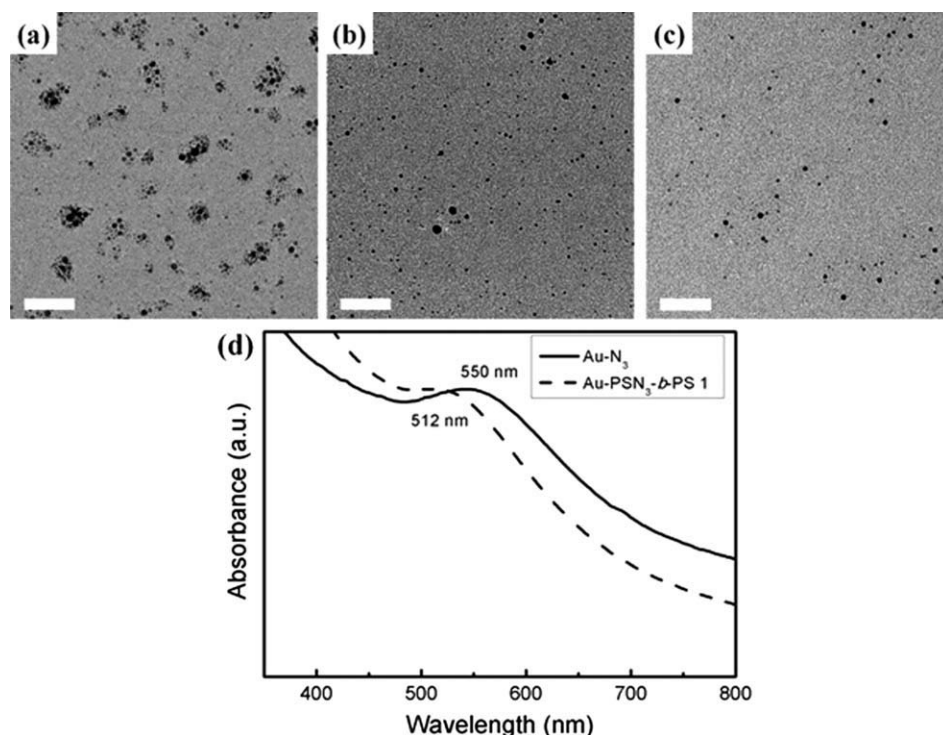


**FIGURE 5** TEM images and the corresponding absorption spectra of Au NPs in the PS homopolymer matrix. Au-N<sub>3</sub> (a), Au-PS (b), and Au-PSN<sub>3</sub>-*b*-PS 1 (c) were dispersed in PS ( $M_n = 56,500$ ) films, respectively. Both Au-PSN<sub>3</sub>-*b*-PS 1 and Au-PS particles after the click reaction were well dispersed in the PS matrix with the absorption peak at 512 nm, but Au-N<sub>3</sub> nanoparticles showed red-shifted absorption spectra at 550 nm (d), which indicates the aggregation of Au-N<sub>3</sub> nanoparticles. Scale bar is 50 nm.

of alkyne-PS-*b*-PS ( $M_n = 8.8$  kg/mol) used in the polymer shell of Au-PSN<sub>3</sub>-*b*-PS 1. The synthesized Au-PSN<sub>3</sub>-*b*-PS 2 showed similar core size of 2.5 nm [Fig. 2(d)], but the  $\Sigma$  value of Au-PSN<sub>3</sub>-*b*-PS 2 particles was much lower ( $\sim 0.9$  chains/nm<sup>2</sup>) than that of Au-PSN<sub>3</sub>-*b*-PS 1 particles.

#### Investigation on Behavior of Polymer-Coated Au NPs in a Polymer Matrix

The morphology of Au NPs in a PS matrix was examined by TEM to investigate the effect of the polymer shell. The blend sample of Au NPs and PS matrix was prepared by mixing both Au NPs ( $\sim 10$  wt %) and PS ( $M_n = 56.5$  kg/mol, PDI = 1.07) in toluene and stirred for several hours. The solutions were drop- or spun-cast on NaCl substrates and the solvent was evaporated slowly at room temperature under ambient conditions without further thermal annealing. To characterize the samples by TEM, the films on NaCl were transferred onto the TEM grid by floating them onto water. Figure 5 represents TEM images of three different Au NPs [(a) Au-N<sub>3</sub>, (b) Au-PS, and (c) Au-PSN<sub>3</sub>-*b*-PS 1] dispersed in PS films. The Au-PSN<sub>3</sub>-*b*-PS 1 and Au-PS particles after click reaction were well dispersed in the PS matrix, whereas the Au-N<sub>3</sub> nanoparticles aggregated because of incompatibility between the particles and the PS matrix. The morphology of the thin films observed by TEM was further supported by UV-Vis absorption measurements [Fig. 5(d)]. The wavelengths of light absorbed by gold nanoparticles are highly sensitive to the particle size and distance between neighboring particles.<sup>56</sup> When Au NPs come into close contact, the absorption wavelength is red-shifted because induced dipoles can further dampen the electron oscillation.<sup>57</sup> UV-Vis absorption spectra of both Au-PS and Au-PSN<sub>3</sub>-*b*-PS 1 in the PS matrix exhibited the peak at 512 nm, which was consistent with the peak in

the solution state. In contrast, Au-N<sub>3</sub> particles in the matrix showed red-shifted absorption spectra at 550 nm, which confirmed the aggregation of Au-N<sub>3</sub> nanoparticles as found in the TEM image. Therefore, it can be concluded that the CuAAC reaction between the Au particle surface and the alkyne polymer chains was successfully performed to form densely packed polymer chains as the shell on the Au NP surface. The presence of well-packed polymer chains was further evidenced by the thermal stability test shown in Figure 6. To enhance the thermal stability, azide groups that can be easily crosslinked by thermal annealing and/or UV irradiation were introduced into Au-PSN<sub>3</sub>-*b*-PS 1 particles. Two different Au-PS and Au-PSN<sub>3</sub>-*b*-PS 1 nanoparticles were embedded in the PS matrix and annealed at the elevated temperature of 200 °C for 24 h. It is well known that because of fragile bonding between the sulfur atoms at the end of the polymer chain and Au atoms on the particle, Au NPs become unstable and aggregate above 60 °C.<sup>33,58</sup> Therefore, after annealing at the elevated temperature of 200 °C, TEM images in Figure 6(a) show that the Au-PS particles became aggregated, showing a dramatic increase in the particle size from 2.5 to 8.5 nm. In contrast, the size of Au-PSN<sub>3</sub>-*b*-PS 1 particles remained unchanged after annealing at 200 °C for 24 h, thus indicating that the PSN<sub>3</sub>-*b*-PS chains were closely packed enough to form the crosslinked shell on the Au NP surface.

To further prove the importance of our approach for the synthesis of Au NPs with highly packed polymer shells via the combined “click” method and RAFT polymerization, polymer nanocomposites consisting of Au-PSN<sub>3</sub>-*b*-PS 1 nanoparticles and lamellar-forming PS-*b*-poly(2-vinylpyridine) (PS-*b*-P2VP matrix;  $M_n = 380$  kg/mol) were prepared on NaCl substrates and annealed at the elevated temperature of 220 °C under

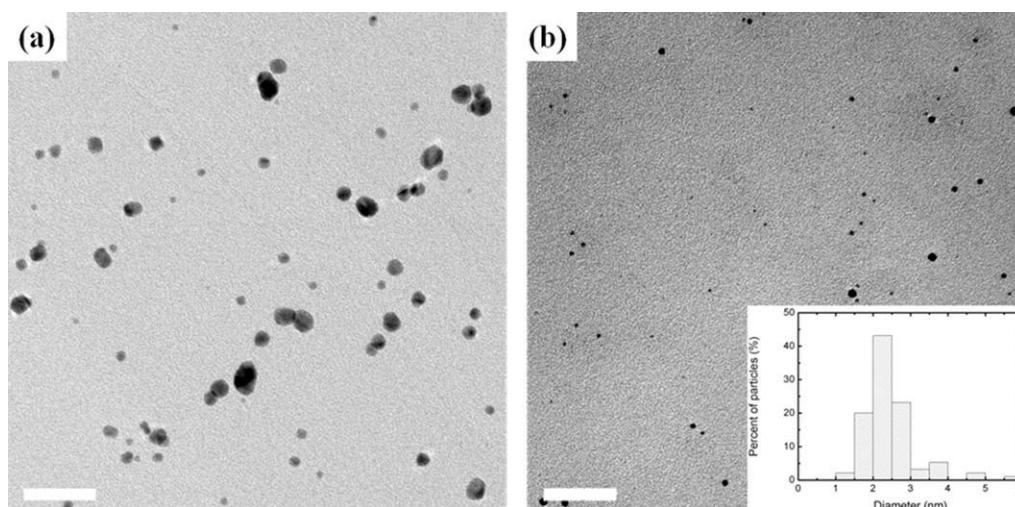


**FIGURE 6** TEM images represent two different nanoparticles (Au-PS and Au-PSN<sub>3</sub>-*b*-PS 1) in the PS matrix annealed at the elevated temperature of 200 °C for 24 h. (a) The Au-PS particles were aggregated and the particle size dramatically increased from 2.5 to 8.5 nm. In contrast, the size of Au-PSN<sub>3</sub>-*b*-PS 1 particles shown in (b) was unchanged because of the presence of azide crosslinkable groups in Au-PSN<sub>3</sub>-*b*-PS 1 particles, thus indicating that the PSN<sub>3</sub>-*b*-PS chains were packed closely enough to form the crosslinked shell on the AuNP surface. Scale bar is 50 nm.

high vacuum ( $\sim 10^{-7}$  Torr). Figure 7 shows cross-sectional TEM images of PS-*b*-P2VP containing Au-PSN<sub>3</sub>-*b*-PS 1 nanoparticles. These images revealed the well-ordered lamellar phase of PS-*b*-P2VP containing the Au NPs without any aggregation. The particles were found to be within PS domain (seen as the brighter area) and at the PS/P2VP interface as shown in the TEM image and the corresponding histogram. It was reported that, because of the favorable interaction between bare Au surfaces and the P2VP matrix, the  $\Sigma$  value is an important parameter for controlling the location of the polymer-coated Au NPs within the block copolymer matrix.<sup>17</sup> According to the previous report,<sup>54</sup> the  $\Sigma$  value of Au-PSN<sub>3</sub>-*b*-PS 1 is above the critical areal chain density that causes the transition of particles from the PS domain to the PS/P2VP interface. However, it should be noted that because of the presence of the azide shell between the

PS shell and the Au NP surface, the  $\Sigma$  effect on the location of our Au-PSN<sub>3</sub>-*b*-PS 1 nanoparticles cannot be directly interpreted by the previous results.<sup>59</sup> We believe that well-dispersed Au-PSN<sub>3</sub>-*b*-PS 1 particles in both the PS and the PS-*b*-P2VP matrices with extremely high thermal stability proved the importance of our approach for the synthesis of Au NPs with highly grafted polymer shells via combining the click method and RAFT polymerization.

## EXPERIMENTAL

### Synthesis of Au-N<sub>3</sub> Nanoparticles

#### Synthesis of 11-(Bromoundecyl)thioacetate (1)

11-Bromo-1-undecene (2.0 g, 8.58 mmol), thioacetic acid (3.1 mL, density = 1.065 g/mL, 42.9 mmol), and azobisisobutyronitrile (AIBN) (704 mg, 4.29 mmol) were dissolved in

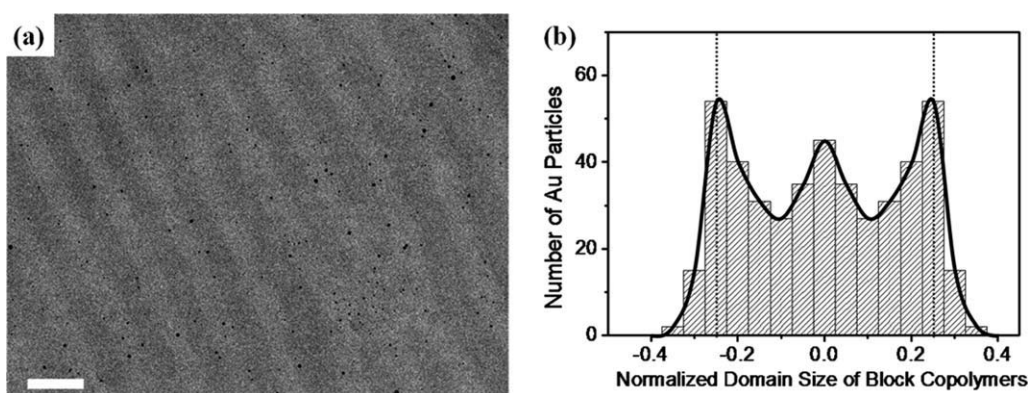


**FIGURE 7** (a) Cross-sectional TEM images of lamellar forming PS-*b*-P2VP block copolymer containing thermally stable PS-coated gold nanoparticles (Au-PSN<sub>3</sub>-*b*-PS 1,  $\Sigma = 1.22$  chains/nm<sup>2</sup>) prepared by the click approach.  $M_n$  of PS-*b*-P2VP = 380 kg/mol. Samples were annealed at 220 °C for 2 days. Scale bar is 100 nm. (b) Histogram of particle positions from the corresponding TEM micrograph. Interfaces of the PS domain are at -0.25 and +0.25, and data are averaged at a given position relative to zero.

toluene (50 mL) under Ar atmosphere. The mixture was stirred at the reflux temperature for 4 h. The resulting mixture was diluted with Et<sub>2</sub>O (200 mL) and the separated organic layer was washed with water ( $\times 3$ ) and brine, dried over MgSO<sub>4</sub>, and concentrated *in vacuo*. The crude product was purified by column chromatography on silica gel using hexane:CH<sub>2</sub>Cl<sub>2</sub> (2:1) as the eluent to yield product **1** (2.31 g, 87%) as a colorless oil. <sup>1</sup>H NMR (CDCl<sub>3</sub>, 500 MHz)  $\delta$  3.40 (t,  $J = 6.7$  Hz, 2H), 2.86 (t,  $J = 7.3$  Hz, 2H), 2.32 (s, 3H), 1.82–1.88 (m, 2H), 1.53–1.59 (m, 2H), 1.27–1.43 (m, 14H).

#### Synthesis of 11-Bromo-1-undecanethiol (**2**)

Compound **1** (1.0 g, 3.23 mmol) was dissolved in anhydrous methanol. Acetyl chloride (2.3 mL, 32.3 mmol) was then added dropwise to the solution under Ar atmosphere and at 0 °C. The subsequent solution was allowed to warm to room temperature for 3 h, and the resulting mixture was diluted with Et<sub>2</sub>O (60 mL). The separated organic layer was washed with water ( $\times 3$ ) and brine, dried over MgSO<sub>4</sub>. The combined organic layer was concentrated under vacuum to give product **2** (786 mg, 91%) as a colorless oil. <sup>1</sup>H NMR (CDCl<sub>3</sub>, 500 MHz)  $\delta$  3.38 (t,  $J = 6.8$  Hz, 2H), 2.49 (q,  $J = 7.6$  Hz, 2H), 1.82–1.88 (m, 2H), 1.53–1.62 (m, 2H), 1.20–1.45 (m, 14H).

#### Synthesis of Bromoundecanethiolate Au NPs (Au-Br, **3**)

The Au NPs were synthesized according to the Schiffrin–Brust method using 0.5 mmol of HAuCl<sub>4</sub>·3H<sub>2</sub>O (aqueous solution, 20 mL), 0.5 mmol of thiol compound **2**, 0.5 mmol of tetraoctylammonium bromide, and 5 mmol of NaBH<sub>4</sub>.<sup>60</sup> Synthesized Au NPs were washed three times with methanol to remove residual ligands and reducing agents.

#### Azidation of the Au NPs (Au-N<sub>3</sub>, **4**)

The Au NPs (70 mg) **3** in dichloromethane (DCM) (15 mL) were added to a solution of NaN<sub>3</sub> (175 mg) in DMSO (15 mL). The solution was stirred for 2 days under N<sub>2</sub> atmosphere at room temperature. After water was added, the black organic layer was isolated and dried over MgSO<sub>4</sub>. The Au NPs were washed with methanol and dried under vacuum.

#### Synthesis of Alkyne-Terminated RAFT Chain Transfer Agent

##### Synthesis of Trithiocarbonate RAFT Agent (**5**)

Trithiocarbonate RAFT Agent **5** was synthesized according to modified literature procedures.<sup>61</sup> 50% aqueous NaOH solution (16 g, 200 mmol) was added to a mixture of 1-butanethiol (18 g, 200 mmol) and water (30 mL), followed by 10 mL acetone and resulted in a colorless solution. The solution was stirred at room temperature for 0.5 h. Carbon disulfide (13.5 mL, 1.27 g/mL, 225 mmol) was added to the resulting solution to obtain a clear orange solution. The reaction mixture was stirred for 0.5 h and then cooled in an ice bath. The 2-bromopropionic acid (31.14 g, 205.0 mmol) was added dropwise, followed by 16 g of 50% aqueous NaOH solution at a rate to keep the temperature of the bath below 30 °C. After the completion of the exothermic reaction, water (80 mL) was added and then the reaction was stirred at room temperature for 24 h. Then, 10 M aqueous HCl (30 mL) was added slowly at 0 °C until solidification. The

solid was separated by filtration, washed with cold water, and dried. Finally, the products were recrystallized from hexane with gentle stirring to give bright yellow solid crystals (34.8 g, 71%). <sup>1</sup>H NMR (CDCl<sub>3</sub>, 500 MHz)  $\delta$  9.90 (br s, 1H), 4.87 (q,  $J = 7.6$  Hz, 1H), 3.37 (t,  $J = 7.3$  Hz, 2H), 1.66–1.72 (m, 2H), 1.64 (d,  $J = 7.6$  Hz, 3H), 1.40–1.47 (m, 2H), 0.94 (t,  $J = 7.3$  Hz, 3H).

##### Alkylation of Trithiocarbonate RAFT Agent (**6**)

Trithiocarbonate RAFT agent (4 g, 16.76 mmol) and DMAP (1.02 g, 8.38 mmol) were dissolved in DCM (200 mL) under N<sub>2</sub> atmosphere. Propargyl alcohol (1.94 mL, 33.52 mmol) was then added, and the mixture was stirred for 15 min at room temperature. Finally, *N,N'*-dicyclohexylcarbodiimide (3.448 g, 16.76 mmol) in DCM (20 mL) was added and allowed to remain at room temperature for 36 h. The reaction product was washed several times with water. After washing, the product was separated by column chromatography. The final product was a yellow oil **6** (4.5g, 97%). <sup>1</sup>H NMR (CDCl<sub>3</sub>, 500 MHz)  $\delta$  4.82 (q,  $J = 7.3$  Hz, 1H), 4.71 (t,  $J = 2.9$  Hz, 2H), 3.34 (t,  $J = 7.3$  Hz, 2H), 2.49 (t,  $J = 2.4$  Hz, 1H), 1.62–1.70 (m, 2H), 1.59 (d,  $J = 7.3$  Hz, 3H), 1.36–1.45 (m, 2H), 0.91 (t,  $J = 7.3$  Hz, 3H).

##### Synthesis of Alkyne-PSCL-*b*-PS (**8**)

Alkyne PSCL-*b*-PS block copolymers were synthesized by RAFT polymerization [Scheme 2(b)]. 4-Vinylbenzylchloride monomer (Aldrich), alkyne-terminated RAFT agent **6**, and AIBN were added into a glass ampoule. The reactants were degassed by three freeze–thaw cycles. The inhibitors in the monomers were removed by an alumina column prior to polymerization, which was performed under vacuum at 70 °C for 24 h. Poly(4-benzylchloride) was then precipitated by cold methanol. Poly(4-benzylchloride), styrene monomer, and AIBN (mol of alkyne-terminated RAFT agent: mol of AIBN = 10:1) in benzene were added into a glass ampoule for sequential polymerization under vacuum. After 24 h reaction at 70 °C, the products were precipitated in cold methanol, filtered, and dried. The total  $M_n$  and PDI of PS-*b*-PSN<sub>3</sub> were determined by SEC, which was calibrated by PS standards. Details of the synthesized polymers are given in Table 1.

##### “Click” Reactions Between Au-N<sub>3</sub> with Alkyne-PSCL-*b*-PS (**9**)

The Au-N<sub>3</sub> particles **4** and alkyne-PSCL-*b*-PS **8** were dissolved in THF. CuSO<sub>4</sub> (2 equiv. per alkyne polymers in water) was added at room temperature, followed by the dropwise addition of sodium ascorbate (5 equiv. per alkyne polymers in water). Argon gas was bubbled through the reaction mixture over 10 min. Final ratio of water to THF was kept at 1:4 to optimize the click reaction. The mixture was stirred under Ar for 2 days at room temperature. Then, DCM and aqueous ammonia solution were added to separate and draw residual copper into the aqueous solution. The organic layer was washed twice with water, dried with MgSO<sub>4</sub>, and the solvent was evaporated under vacuum. The resulting solid was redispersed in CH<sub>2</sub>Cl<sub>2</sub> and precipitated in ethanol and methanol. It was subsequently centrifuged at 18,000 rpm several times using a gradient mixture of DCM and

cyclohexane to remove unreacted polymers and residuals. Then, Au-PSCI-*b*-PS (172.6 mg) and sodium azide (220 mg) were dissolved in DMF and stirred for 24 h. Finally, Au NPs were purified by centrifugation.

### Characterization

NMR spectra were obtained by Bruker AMX 500. FTIR spectra were taken on a Bruker IFS66V/S & HYPERION 3000. The  $M_n$  and PDI of synthesized polymers were obtained by SEC using a Waters 1515 pump and a Waters 2414 differential refractometer in THF at 35 °C with a flow rate of 1 mL/min. SEC was calibrated by PS standards. TGA was performed on a TA Q500 at a scan rate of 10 °C/min from room temperature to 600 °C under N<sub>2</sub> atmosphere.

The characterization of Au NPs was carried out using TEM, NMR, FTIR, GPC, UV-Vis, and TGA. The core size of Au NPs was analyzed by TEM (Tecnai G220 S-twin or JEOL JEL-3011 HR) images. A carbon-coated TEM grid was dipped into a dilute solution of Au NPs for several seconds and dried under air before being examined by TEM. The weight fraction of gold and organic ligands in the core-shell Au NPs was analyzed by TGA. The weight fraction of polymer brushes and gold particles were converted to volume fraction using the density of organic ligands and the density of the gold particles (~19.3 g/cm<sup>3</sup>). It should be noted that the ungrafted organic and/or polymer ligands were washed several times by centrifugation. Polymer ligands were carefully washed several times by centrifugation using the density-gradient method,<sup>62,63</sup> in which the particles were washed through five different layers of DCM and cyclohexane at various ratios with different densities. The unwashed alkyne-terminated polymer after each washing step was monitored by SEC. The grafting density of polymer ligands on the Au NPs was estimated by dividing the number of ligands attached on Au surface by the surface area.

### CONCLUSIONS

In this work, we developed a simple and powerful route for creating thermally stable core-shell gold nanoparticles with highly grafted polymer shells by combining RAFT and click chemistry. Properly designed diblock copolymer of PS and PSCI with alkyne end group was coupled to Au-N<sub>3</sub> by CuAAC reaction, in which the reaction conditions such as ratio of THF/water during reaction was carefully optimized, thereby achieving good solubility of all reagents including the Cu catalyst and salt. Careful characterization using FTIR, UV-Vis, and TGA showed that PSN<sub>3</sub>-*b*-PS chains were successfully grafted onto the Au NP surface with high grafting density. The synthesized Au NPs exhibited good thermal stability over 220 °C because of the densely grafted and crosslinked PSN<sub>3</sub> blocks in polymer shell. We successfully demonstrated the importance of our highly packed polymer shell on the nanoparticles by examining their behavior in homopolymer and diblock copolymer matrix. We believe that this approach can be easily extended to design other functional core-shell nanoparticles.

This work was supported by the National Research Foundation of Korea Grant funded by the Korean Government (2009-0085070, 2009-0088551, 2010-0011033, and 2010-0016304).

### REFERENCES AND NOTES

- 1 Beecroft, L. L.; Ober, C. K. *Chem Mater* 1997, 9, 1302–1317.
- 2 Sanchez, C.; Lebeau, B.; Chaput, F.; Boilot, J. P. *Adv Mater* 2003, 15, 1969–1994.
- 3 Sohn, B. H.; Cohen, R. E. *J Appl Polym Sci* 1997, 65, 723–729.
- 4 Buxton, G. A.; Balazs, A. C. *Mol Simul* 2004, 30, 249–257.
- 5 Zijlstra, P.; Chon, J. W. M.; Gu, M. *Nature* 2009, 459, 410–413.
- 6 Siwick, B. J.; Kalinina, O.; Kumacheva, E.; Miller, R. J. D.; Noolandi, J. *J Appl Phys* 2001, 90, 5328–5334.
- 7 Tsutsumi, K.; Funaki, Y.; Hirokawa, Y.; Hashimoto, T. *Langmuir* 1999, 15, 5200–5203.
- 8 Zalusky, A. S.; Olayo-Valles, R.; Wolf, J. H.; Hillmyer, M. A. *J Am Chem Soc* 2002, 124, 12761–12773.
- 9 Mackay, M. E.; Tuteja, A.; Duxbury, P. M.; Hawker, C. J.; Van Horn, B.; Guan, Z. B.; Chen, G. H.; Krishnan, R. S. *Science* 2006, 311, 1740–1743.
- 10 Bockstaller, M. R.; Lapetnikov, Y.; Margel, S.; Thomas, E. L. *J Am Chem Soc* 2003, 125, 5276–5277.
- 11 Huang, C. M.; Wei, K. H. *Macromolecules* 2008, 41, 6876–6879.
- 12 Kang, H.; Detcheverry, F. A.; Mangham, A. N.; Stoykovich, M. P.; Daoulas, K. C.; Hamers, R. J.; Muller, M.; de Pablo, J. J.; Nealey, P. F. *Phys Rev Lett* 2008, 100, 148303-1–148303-4.
- 13 Maria, S.; Susha, A. S.; Sommer, M.; Talapin, D. V.; Rogach, A. L.; Thelakkat, M. *Macromolecules* 2008, 41, 6081–6088.
- 14 Li, Q. F.; He, J. B.; Glogowski, E.; Li, X. F.; Wang, J.; Emrick, T.; Russell, T. P. *Adv Mater* 2008, 20, 1462–1466.
- 15 Lin, Y.; Boker, A.; He, J. B.; Sill, K.; Xiang, H. Q.; Abetz, C.; Li, X. F.; Wang, J.; Emrick, T.; Long, S.; Wang, Q.; Balazs, A.; Russell, T. P. *Nature* 2005, 434, 55–59.
- 16 Chung, H.; Ohno, K.; Fukuda, T.; Composto, R. J. *Nano Lett* 2005, 5, 1878–1882.
- 17 Kim, B. J.; Bang, J.; Hawker, C. J.; Kramer, E. J. *Macromolecules* 2006, 39, 4108–4114.
- 18 Kim, B. J.; Chiu, J. J.; Yi, G. R.; Pine, D. J.; Kramer, E. J. *Adv Mater* 2005, 17, 2618–2622.
- 19 Listak, J.; Bockstaller, M. R. *Macromolecules* 2006, 39, 5820–5825.
- 20 Spontak, R. J.; Shankar, R.; Bowman, M. K.; Krishnan, A. S.; Hamersky, M. W.; Samseth, J.; Bockstaller, M. R.; Rasmussen, K. O. *Nano Lett* 2006, 6, 2115–2120.
- 21 Lan, Q.; Francis, L. F.; Bates, F. S. *J Polym Sci Part B: Polym Phys* 2007, 45, 2284–2299.
- 22 Xu, C.; Ohno, K.; Ladmiral, V.; Composto, R. J. *Polymer* 2008, 49, 3568–3577.

- 23** Chiu, J. J.; Kim, B. J.; Kramer, E. J.; Pine, D. J. *J Am Chem Soc* 2005, 127, 5036–5037.
- 24** van Berkel, K. Y.; Hawker, C. J. *J Polym Sci Part A: Polym Chem* 2010, 48, 1594–1606.
- 25** Kim, B. J.; Bang, J.; Hawker, C. J.; Chiu, J. J.; Pine, D. J.; Jang, S. G.; Yang, S. M.; Kramer, E. J. *Langmuir* 2007, 23, 12693–12703.
- 26** Kim, J. S.; Jeon, H. J.; Park, J. J.; Park, M. S.; Youk, J. H. *J Polym Sci Part A: Polym Chem* 2009, 47, 4963–4970.
- 27** Vestberg, R.; Piekarski, A. M.; Pressly, E. D.; Van Berkel, K. Y.; Malkoch, M.; Gerbac, J.; Ueno, N.; Hawker, C. J. *J Polym Sci Part A: Polym Chem* 2009, 47, 1237–1258.
- 28** Kim, B. J.; Fredrickson, G. H.; Bang, J.; Hawker, C. J.; Kramer, E. J. *Macromolecules* 2009, 42, 6193–6201.
- 29** Corbierre, M. K.; Cameron, N. S.; Sutton, M.; Laaziri, K.; Lennox, R. B. *Langmuir* 2005, 21, 6063–6072.
- 30** Corbierre, M. K.; Cameron, N. S.; Lennox, R. B. *Langmuir* 2004, 20, 2867–2873.
- 31** Luo, S. Z.; Xu, J.; Zhu, Z. Y.; Wu, C.; Liu, S. Y. *J Phys Chem B* 2006, 110, 9132–9139.
- 32** Zhu, M. Q.; Wang, L. Q.; Exarhos, G. J.; Li, A. D. Q. *J Am Chem Soc* 2004, 126, 2656–2657.
- 33** Xiao, X. D.; Wang, B.; Zhang, C.; Yang, Z.; Loy, M. M. T. *Surf Sci* 2001, 472, 41–50.
- 34** Kolb, H. C.; Finn, M. G.; Sharpless, K. B. *Angew Chem Int Ed Engl* 2001, 40, 2004–2021.
- 35** Rostovtsev, V. V.; Green, L. G.; Fokin, V. V.; Sharpless, K. B. *Angew Chem Int Ed Engl* 2002, 41, 2596–2599.
- 36** Magenau, A. J. D.; Martinez-Castro, N.; Savin, D. A.; Storey, R. F. *Macromolecules* 2009, 42, 8044–8051.
- 37** Pressly, E. D.; Amir, R. J.; Hawker, C. J. *J Polym Sci Part A: Polym Chem* 2011, 49, 814–819.
- 38** Collman, J. P.; Devaraj, N. K.; Eberspacher, T. P. A.; Chidsey, C. E. D. *Langmuir* 2006, 22, 2457–2464.
- 39** Ru, X.; Zeng, X. H.; Li, Z. M.; Evans, D. J.; Zhan, C. X.; Tang, Y.; Wang, L. J.; Liu, X. M. *J Polym Sci Part A: Polym Chem* 2010, 48, 2410–2417.
- 40** Lee, L. V.; Mitchell, M. L.; Huang, S. J.; Fokin, V. V.; Sharpless, K. B.; Wong, C. H. *J Am Chem Soc* 2003, 125, 9588–9589.
- 41** Hein, J. E.; Fokin, V. V. *Chem Soc Rev* 2010, 39, 1302–1315.
- 42** Brennan, J. L.; Hatzakis, N. S.; Tshikhudo, T. R.; Dirvian-skyte, N.; Razumas, V.; Patkar, S.; Vind, J.; Svendsen, A.; Nolte, R. J. M.; Rowan, A. E.; Brust, M. *Bioconjugate Chem* 2006, 17, 1373–1375.
- 43** Ranjan, R.; Brittain, W. J. *Macromolecules* 2007, 40, 6217–6223.
- 44** Fischler, M.; Sologubenko, A.; Mayer, J.; Clever, G.; Burley, G.; Gierlich, J.; Carell, T.; Simon, U. *Chem Commun* 2008, 169–171.
- 45** Fleming, D. A.; Thode, C. J.; Williams, M. E. *Chem Mater* 2006, 18, 2327–2334.
- 46** Drockenmuller, E.; Colinet, I.; Dameron, D.; Gal, F.; Perez, H.; Carrot, G. *Macromolecules* 2010, 43, 9371–9375.
- 47** Boisselier, E.; Salmon, L.; Ruiz, J.; Astruc, D. *Chem Commun* 2008, 5788–5790.
- 48** Zhang, T.; Zheng, Z. H.; Ding, X. B.; Peng, Y. X. *Macromol Rapid Commun* 2008, 29, 1716–1720.
- 49** Yoo, M.; Kim, S.; Lim, J.; Kramer, E. J.; Hawker, C. J.; Kim, B. J.; Bang, J. *Macromolecules* 2010, 43, 3570–3575.
- 50** Terrill, R. H.; Postlethwaite, T. A.; Chen, C. H.; Poon, C. D.; Terzis, A.; Chen, A. D.; Hutchison, J. E.; Clark, M. R.; Wignall, G.; Londono, J. D.; Superfine, R.; Falvo, M.; Johnson, C. S.; Samulski, E. T.; Murray, R. W. *J Am Chem Soc* 1995, 117, 12537–12548.
- 51** Badia, A.; Gao, W.; Singh, S.; Demers, L.; Cuccia, L.; Reven, L. *Langmuir* 1996, 12, 1262–1269.
- 52** Li, Z.; Zhang, K.; Ma, J.; Cheng, C.; Wooley, K. L. *J Polym Sci Part A: Polym Chem* 2009, 47, 5557–5563.
- 53** Tao, L.; Kaddis, C. S.; Loo, R. R. O.; Grover, G. N.; Loo, J. A.; Maynard, H. D. *Chem Commun* 2009, 2148–2150.
- 54** Kim, B. J.; Fredrickson, G. H.; Kramer, E. J. *Macromolecules* 2008, 41, 436–447.
- 55** Kim, B. J.; Given-Beck, S.; Bang, J.; Hawker, C. J.; Kramer, E. J. *Macromolecules* 2007, 40, 1796–1798.
- 56** LizMarzan, L. M.; Giersig, M.; Mulvaney, P. *Langmuir* 1996, 12, 4329–4335.
- 57** Ung, T.; Liz-Marzan, L. M.; Mulvaney, P. *J Phys Chem B* 2001, 105, 3441–3452.
- 58** Ramachandran, G. K.; Hopson, T. J.; Rawlett, A. M.; Nagahara, L. A.; Primak, A.; Lindsay, S. M. *Science* 2003, 300, 1413–1416.
- 59** Jang, S. G.; Khan, A.; Dimitriou, M.; Kim, B. J.; Lynd, N. A.; Kramer, E. J.; Hawker, C. J. *Soft Matter*, in press; DOI: 10.1039/c1sm05223c.
- 60** Brust, M.; Walker, M.; Bethell, D.; Schiffrin, D. J.; Whyman, R. *J Chem Soc Chem Commun* 1994, 801–802.
- 61** Ferguson, C. J.; Hughes, R. J.; Nguyen, D.; Pham, B. T. T.; Gilbert, R. G.; Serelis, A. K.; Such, C. H.; Hawker, B. S. *Macromolecules* 2005, 38, 2191–2204.
- 62** Bai, L.; Ma, X. J.; Liu, J. F.; Sun, X. M.; Zhao, D. Y.; Evans, D. G. *J Am Chem Soc* 2010, 132, 2333–2337.
- 63** Kwon, T.; Min, M.; Lee, H.; Kim, B. J. *J Mater Chem*, in press; DOI:10.1039/C1JM11318F.